AER/AGS Open File Report 2019-02

Induced Earthquake Geological Susceptibility Model for the Duvernay Formation, Central Alberta – Version 2

AER/AGS Open File Report 2019-02

Induced Earthquake Geological Susceptibility Model for the Duvernay Formation, Central Alberta – Version 2

R. Schultz and S. Pawley

Alberta Energy Regulator
Alberta Geological Survey

June 2019

ISBN 978-1-4601-3989-9

If you use information from this publication in other publications or presentations, please acknowledge the AER/AGS. We recommend the following reference format:

Schultz, R. and Pawley, S.M. (2019): Induced earthquake geological susceptibility model for the Duvernay Formation, central Alberta – version 2; Alberta Energy Regulator / Alberta Geological Survey, AER/AGS Open File Report 2019-02, 8 p.

Publications in this series have undergone only limited review and are released essentially as submitted by the author.

Published June 2019 by:
Alberta Energy Regulator
Alberta Geological Survey
4th Floor, Twin Atria Building
4999 – 98th Avenue
Edmonton, AB T6B 2X3
Canada

Tel: 780.638.4491
Fax: 780.422.1459
Email: AGS-Info@aer.ca
Website: www.ags.aer.ca

Contents

Figures

Abstract

This report presents the second iteration of a geological susceptibility model for estimating the potential for induced seismicity in the Duvernay Formation of central Alberta. It documents the changes made to the first version of the model to more faithfully represent the induced seismicity situation in central Alberta. This second version includes updates to the observed seismogenic clusters, including two in the newly emerging East Shale Basin of the Duvernay Formation. As well, a new input feature (proximity to the Leduc Formation) is included in the analysis. Slight methodology tweaks were made to implement a mixed L_1/L_2 (lasso/ridge) regularization, and to better capture the geometry of horizontal wells. Overall, the new model recovers many attributes of the previous version and performs slightly better.

Previously, geological data was used as input features and wells assigned as seismic/aseismic to train a machine learning algorithm to evaluate tectonic, geomechanical, and hydrological proxies suspected of controlling induced seismicity. However, the initial model was limited by a lack of subsurface geological information, a restricted number of developed wells, and a paucity of induced earthquake clusters.

The first version of the model was published as

> Pawley, S., Schultz, R., Playter, T., Corlett, H., Shipman, T., Lyster, S. and Hauck, T. (2018): The geological susceptibility of induced earthquakes in the Duvernay play; Geophysical Research Letters, v. 45, issue 4, p. 1786–1793, doi:10.1002/2017GL076100.

1 Introduction

The Western Canada Sedimentary Basin has witnessed an increase in the earthquake rate, which has been attributed to petroleum resource development (Atkinson et al., 2016). In particular, hydraulic fracturing has contributed most significantly to the apparent rate change in the past few years (e.g., Schultz et al., 2017, 2018). Despite the regionally pronounced change in seismicity rate and the associated hazards (Ghofrani et al., 2019), only a small proportion of the wells within the Western Canada Sedimentary Basin are associated with induced earthquakes (Atkinson et al., 2016). Complications with rate and location models have presented difficulties in developing forecasts of induced earthquakes and their hazards.

However, in some cases, geological proxies (Ghofrani and Atkinson, 2016; Schultz et al., 2016; Corlett et al., 2018; Eaton and Schultz, 2018; Galloway et al., 2018; Kao et al., 2018; Skoumal et al., 2018) have been successfully used to provide first-order explanations of potential induced seismicity locations. Often, these proxies indicate underlying conditions responsible for allowing fault slip. Furthermore, operational factors, such as completion volume, have been successful in quantifying changes in earthquake rates (Hincks et al., 2018; Schultz et al., 2018). Within this operational framework, the geological factors related to well locations were found to have a significant impact on the absence/presence of induced earthquakes.

Taking these ideas further, the geological susceptibility approach used a machine learning method to systematically evaluate any geological proxies thought to contribute to the seismogenic process (Pawley et al., 2018). Wells that were and were not associated with induced seismicity were used as training data in a binary classification problem. A logistic regression machine learning algorithm was chosen for its simplicity in quantifying the importance of underlying geological proxies as features in this model. In this approach, the seismogenic activation potential (SAP)—the likelihood of a region encountering induced earthquakes—is estimated statistically. Ongoing results from this work could inform a conceptual understanding of how induced earthquakes occur, what geological conditions are of relative importance, and a guessing of which areas may be prone to future fault reactivation (Pawley et al., 2018).

In practice, the underlying geological features/proxies that control induced earthquake rate and location models are not entirely known, at least in part due to incomplete subsurface databases. Certainly, the first version of the model suffers from this drawback. To combat this, a new version of the induced earthquake geological susceptibility model was constructed. As new information becomes available, the statistical estimates of the seismogenic activation potential (SAP) will become increasingly refined.

This report documents the changes made to the model since the first iteration (Pawley et al., 2018) until now and the rationale for the changes made. As well, this latest update provides a separate table of SAP values at varying confidence intervals.

2 Updates Since Version 1

Changes to the geological susceptibility approach were made between the current and previous model iterations, both in terms of the underlying geological features used and the updates to well training data.

2.1 Methodology

In this version of the geological susceptibility model, the general workflow has remained intact. However, a few minor but notable changes have been made. For example, the original logistic regression classifier utilized L_1 regularization (lasso); the new version employs a mixing between L_1 and L_2 (ridge) regularizations (elastic net regularization, Friedman et al., 2010). This change was implemented as elastic net regularization combines the best aspects of L_1 and L_2 regularization. Ambiguity in the modelling methodology is removed because the relative balance between L_1 and L_2 type regularization is chosen automatically during nested cross-validation. This slight regularization modification also appears to be reflected in the model results, which show a slight improvement in capturing the potential for susceptibility in newly developing regions. Lastly, the coefficients are better at isolating groups of related predictors (as will be described in Section 3).

One additional minor change is the more accurate representation of the lateral geometry of hydraulic fracturing wells. Previously, well locations were considered to be in an area in between the surface and bottom hole locations. Errors were considered by resampling geological features within a 2 km radius around this region. Now well locations are more accurately represented by a lateral length in between the surface and bottom hole locations. More details on the original prescription of the approach can be found in Pawley et al. (2018).

2.2 Input Geological Features

The choice of input geological data/proxies to represent features in the geological susceptibility model was based on those features that demonstrated an influence on the spatial distribution of seismic events in the Duvernay play (Schultz et al., 2016; Eaton and Schultz, 2018): those thought to be related to the seismogenic process, and then restricted to those that are publicly available. In general, any geological features thought to be indications of tectonic structures or faulting, variances in regional effective stress, or hydrological communication along faults were included.

In this current iteration of the geological susceptibility model, one additional change to the input features was implemented. Proximity to the Leduc Formation was included as a potential proxy for faulting and hydraulic communication. The reasoning for this inclusion is similar to the prior rationale used for including proximity to the underlying Swan Hills Formation (Schultz et al., 2016)—that the nucleation and growth of reefs is often influenced by structural controls (Corlett et al., 2018). Ultimately, the choice to incorporate the Leduc Formation as a feature was based on the increased performance of the model (see Section 3). For more information on the features included in the original version, their processing, and inclusion rationale see Pawley et al. (2018).

2.3 Well Training Data

Seismicity throughout the province is ongoing (Stern et al., 2013; Schultz and Stern, 2015). To date, numerous clusters of events have been recognized as a result of secondary recovery (Wetmiller, 1986; Baranova et al., 1999), wastewater disposal (Schultz et al., 2014), and hydraulic fracturing (Schultz et al., 2015a, 2017, 2018; Atkinson et al., 2016). In this approach, wells associated with events larger than the cutoff local magnitude of M_L 2.5 are defined as seismogenic. Note that M_L 2.5 is the approximate magnitude of completeness for the Duvernay play (Schultz et al., 2015b). For more information, see original descriptions of the geological susceptibility approach in Pawley et al. (2018) and Schultz et al. (2018).

Cataloguing induced earthquakes is an ongoing process as new data become available—emerging earthquake clusters are identified and then associated with newly developed wells. The prior version of the geological susceptibility model included available data up until the end of the 2016 calendar year (Pawley et al., 2018). The new version updates this dataset to include data collected up to April 25, 2019 (Figure 1). For Duvernay Formation horizontal hydraulic fracturing wells, this version now includes 1175 wells (previously 833): 1080 aseismic (previously 785) and 95 seismic (previously 48) wells. Noteworthy changes include 13 new clusters, two of which are in a previously unrecognized area of seismicity (i.e., the East Shale Basin). As well, the list of injection wells has been modified to include both disposal and injection wells used for secondary hydrocarbon recovery. This dataset has also been depth filtered to include everything beneath the Banff Formation, as compared to the previous filter that only included wells deeper than the sub-Cretaceous unconformity. Injection and disposal wells are still laterally filtered to include only those within the outline of the Duvernay Formation. The updated injection list includes 1068 wells (previously 365), with no new seismogenic cases identified.

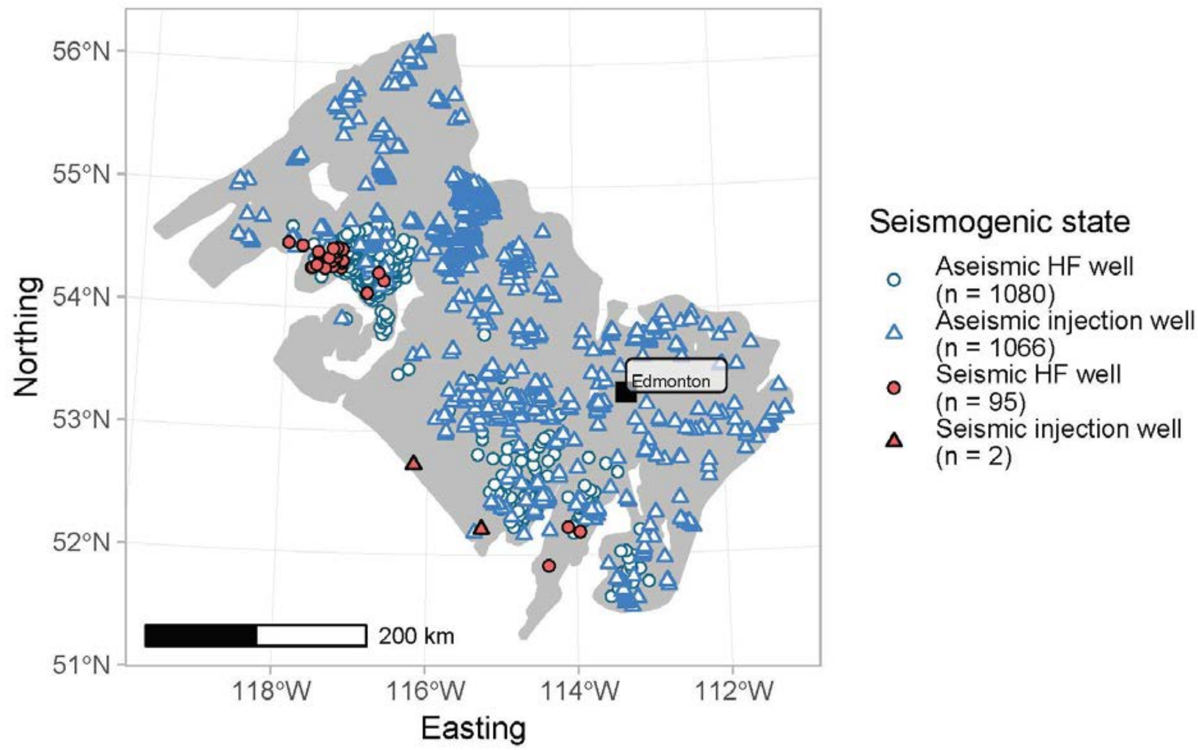

Figure 1. Map of well training data (collected up to April 25, 2019). Training data, used to inform the logistic regression machine learning algorithm, are based on both injection wells (triangles) and multistage horizontal fracturing wells (HF; circles) within the Duvernay Formation (grey outline). A seismogenic state was assigned to each well, either seismic (red) or aseismic (white).

3 Results in Version 2

In general, many of the salient points discussed in the original model (Pawley et al., 2018) are retained in this updated version. Input features still sort themselves into three distinct categories (Figure 2a, farthest from zero to closest to zero): high, medium, and low importance. Similar to the original work, the most important feature is proximity to basement. The medium category sees the same relative importance, with some slight reshuffling of the ordering between features. Some of these potential reshufflings could be the result of including the proximity to the Leduc Formation: many input features are likely covariant with this feature, and this covariance could allow model weight to be shifted off of dependent features and onto the Leduc Formation. Lastly, the use of mixed L_1/L_2 regularization appears to better constrain in situ Duvernay Formation pressure as a positively associated model coefficient now (Figure 2a).

These changes appear to have led to a slight improvement in the global performance of this model: the receiver operator characteristics area under curve (ROC AUC) is slightly higher (Figure 2b) than the initial model (i.e., 0.91 ±0.02 versus 0.87 ±0.02). Overall, the model appears to be producing results that attempt to honour the expected subsurface conditions.

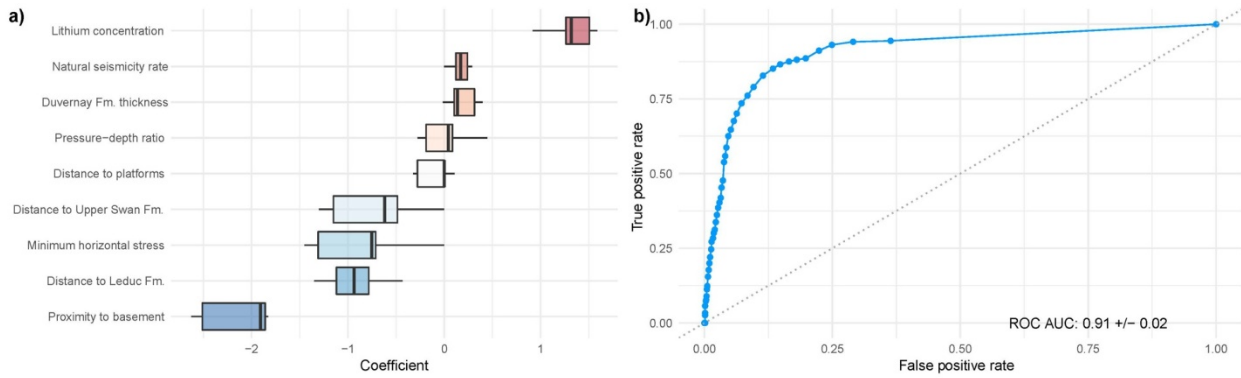

Figure 2. Feature weights and performance of the geological susceptibility model: a) bootstrapped model coefficients signify the relative importance and direction of correlation of input features, and b) the receiver operator characteristics area under curve (ROC AUC) quantifies the performance of these models.

From the perspective of quantifying the SAP at a play-based scale, the output model appears to reiterate many of the same attributes. High susceptibility is observed in the Kaybob area in the northwest and in regions along the Rocky Mountain deformation front in the southwest (Figures 3 and 4). Extrapolation to regions around the Snipe Lake earthquake (west of Valleyview; Milne, 1970) and areas of quarrying south of Hinton still remain speculative. The retention of similar and important attributes in these models signifies some stability in the approach to new data and reworked procedures. This stability is further observed via bootstrap tests in which the input training data are randomly flipped in their association states (Figure 4).

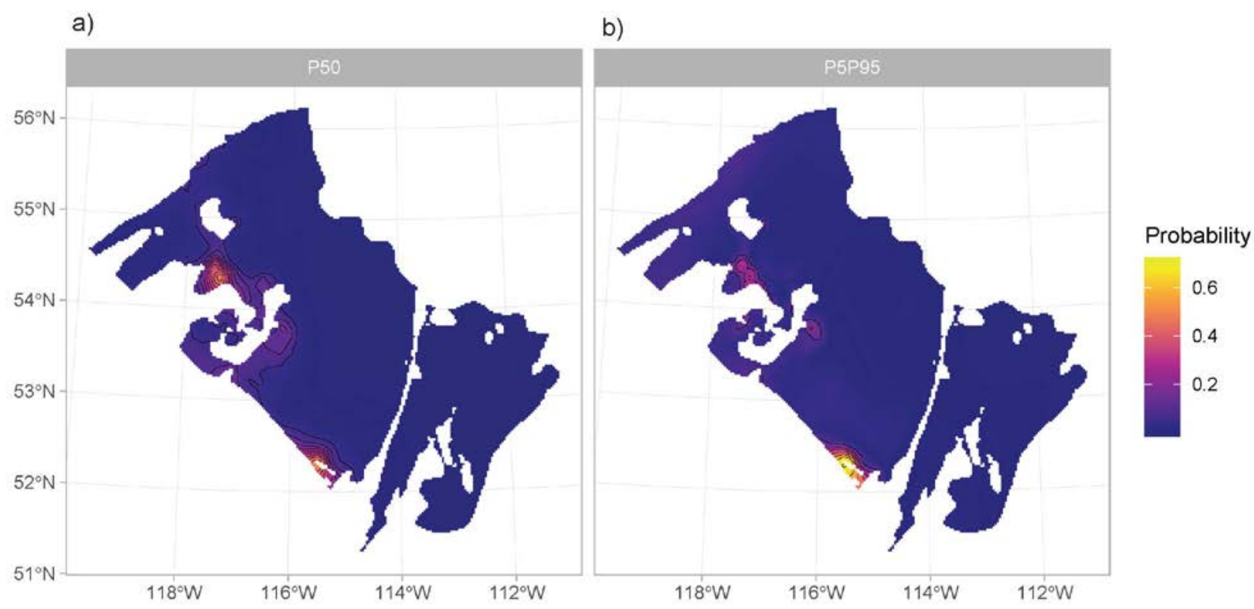

Figure 3. Seismogenic activation potential (SAP) estimates from the current geological susceptibility model (v2): a) median model values of SAP (at the 50th percentile [P50]), and b) error in the SAP (difference between the 5th and 95th percentiles [P5 and P95]).

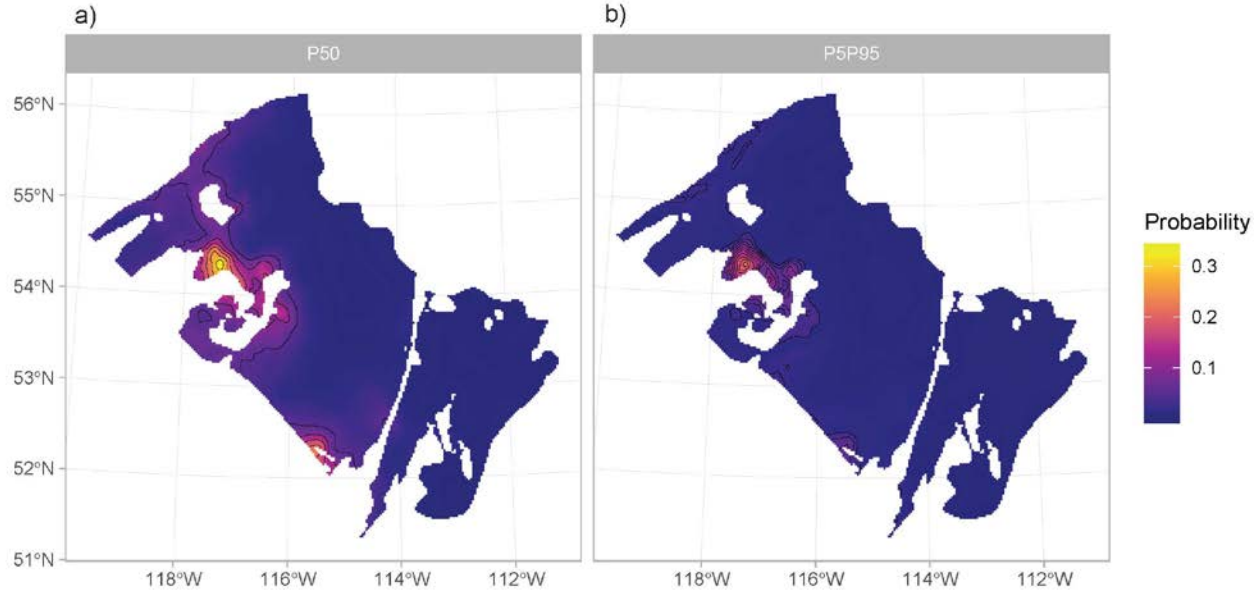

Figure 4. Model sensitivity based on bootstrapped results: a) median model values of bootstrapped seismogenic activation potential (SAP; at the 50th percentile [P50]), and b) error in the bootstrapped SAP (difference between the 5th and 95th percentiles [P5 and P95]).

Next, changes to the updated model were quantified by examining differences and ratios in the SAP (Figure 5). New induced earthquake clusters in the East Shale Basin (to be characterized in upcoming work) are slightly better reflected in this model: SAP in this region is now higher than before (~nine times higher near the deformation front). However, a SAP value lower than values found in highly seismogenic regions (like the Kaybob area) is still observed in the East Shale Basin. This may reflect the reality of the susceptibility here, as only two induced cases exceeded the detection threshold. However, a paucity of hydraulic fracturing completions in this region could hamper a more stable SAP output. Evidence of this is reflected in the higher variability of the model here (Figures 3b and 4b), especially when moving closer to the Rocky Mountain deformation front.

Lastly, the inclusion of proximity to the Leduc Formation appears to have made systematic changes to the extrapolation of the SAP. Higher susceptibilities are silhouetted along the margins of the Leduc Formation, along the southwestern edge of the Duvernay Formation (Figure 5b). Although speculative, this provides increased circumstantial evidence that the Snipe Lake earthquake (Milne, 1970) may have been induced.

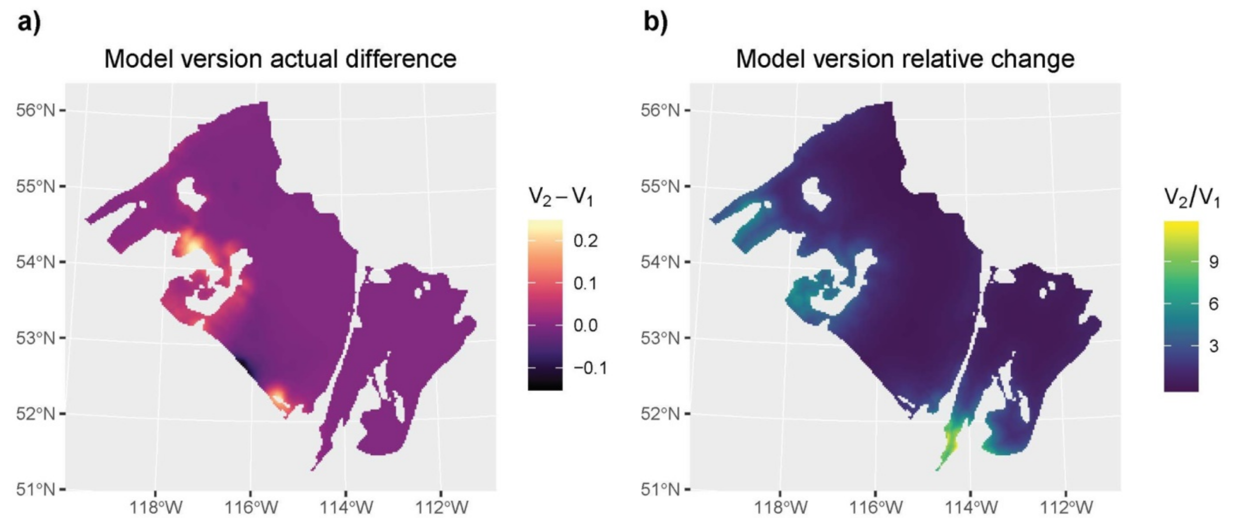

Figure 5. Comparison of the current model (v2) against the prior version (v1): a) difference between median values of seismogenic activation potential (SAP; v2–v1), and b) ratio of median values of SAP (v2/v1).

4 Conclusions

In conclusion, this report outlines the next iteration of the model of geological susceptibility to induced earthquakes in the Duvernay Formation. The model was updated to include 13 new seismogenic cases of induced seismicity, including two within the newly emerging East Shale Basin. Overall, many of the same features and much of the understanding of the subsurface are recovered from the first version with this new increment of data. This suggests the geological susceptibility approach is likely producing results that honour the subsurface conditions. Inclusion of the Leduc Formation places a greater emphasis on regions nearby these platforms, including the seismogenic East Shale Basin. As well, a larger dataset of injection and disposal wells better constrains regions that have been aseismic in the past. Future iterations of this model should become increasingly accurate as the input datasets become increasingly complete.

5 References

Atkinson, G.M., Eaton, D.W., Ghofrani, H., Walker, D., Cheadle, B., Schultz, R., Scherbakov, R., Tiampo, K., Gu., Y.J., Harrington, R.M., Liu, Y., van der Baan, M. and Kao, H. (2016): Hydraulic fracturing and seismicity in the Western Canada Sedimentary Basin; Seismological Research Letters, v. 87, no. 3, p. 631–647, doi:10.1785/0220150263.

Baranova, V., Mustaqeem, A. and Bell, S. (1999): A model for induced seismicity caused by hydrocarbon production in the Western Canada Sedimentary Basin; Canadian Journal of Earth Sciences, v. 36, no. 1, p. 47–64, doi:10.1139/e98-080.

Corlett, H., Schultz, R., Branscombe, P., Hauck, T., Haug, K., MacCormack, K. and Shipman, T. (2018): Subsurface faults inferred from reflection seismic, earthquakes, and sedimentological relationships: implications for induced seismicity in Alberta, Canada; Marine and Petroleum Geology, v. 93, p. 135–144, doi:10.1016/j.marpetgeo.2018.03.008.

Eaton, D.W. and Schultz, R. (2018): Increased likelihood of induced seismicity in highly overpressured shale formations; Geophysical Journal International, v. 214, issue 1, p. 751–757, doi:10.1093/gji/ggy167.

Friedman, J., Hastie, T. and Tibshirani, R. (2010): Regularization paths for generalized linear models via coordinate descent; Journal of Statistical Software, v. 33, issue 1.

Galloway, E., Hauck, T., Corlett, H., Pana, D. and Schultz, R. (2018): Faults and associated karst collapse suggest conduits for fluid flow that influence hydraulic fracturing-induced seismicity; Proceedings of the National Academy of Sciences, v. 115, issue 43, p. E10002–E10013, doi:10.1073/pnas.1807549115.

Ghofrani, H. and Atkinson, G.M. (2016): A preliminary statistical model for hydraulic fracture-induced seismicity in the Western Canada Sedimentary Basin; Geophysical Research Letters, v. 43, issue 19, doi:10.1002/2016GL070042.

Ghofrani, H., Atkinson, G.M., Schultz, R. and Assatourians, K. (2019): Short-term hindcasts of seismic hazard in the Western Canada Sedimentary Basin caused by induced and natural earthquakes; Seismological Research Letters, v. 90, no. 3, p. 1420–1435, doi:10.1785/0220180285.

Hincks, T., Aspinall, W., Cooke, R. and Gernon, T. (2018): Oklahoma's induced seismicity strongly linked to wastewater injection depth; Science, v. 359, issue 6381, p. 1251–1255, doi:10.1126/science.aap7911.

Kao, H., Hyndman, R., Jiang, Y., Visser, R., Smith, B., Babaie Mahani, A., Leonard, L., Ghofrani, H and He, J. (2018): Induced seismicity in western Canada linked to tectonic strain rate: implications for regional seismic hazard; Geophysical Research Letters, v. 45, issue 20, p. 11,104–11,115, doi:10.1029/2018GL079288.

Milne, W.G. (1970): The Snipe Lake, Alberta earthquake of March 8, 1970; Canadian Journal of Earth Sciences, v. 7, no. 6, p. 1564–1567, doi:10.1139/e70-148.

Pawley, S., Schultz, R., Playter, T., Corlett, H., Shipman, T., Lyster, S. and Hauck, T. (2018): The geological susceptibility of induced earthquakes in the Duvernay play; Geophysical Research Letters, v. 45, issue 4, p. 1786–1793, doi:10.1002/2017GL076100.

Schultz, R. and Stern, V. (2015): The Regional Alberta Observatory for Earthquake Studies Network (RAVEN); Canadian Society of Exploration Geophysicists Recorder, v. 40, no. 8, p. 34–37.

Schultz, R., Stern, V. and Gu, Y.J. (2014): An investigation of seismicity clustered near the Cordel Field, west central Alberta, and its relation to a nearby disposal well; Journal of Geophysical Research: Solid Earth, v. 119, issue 4, p. 3410–3423, doi:10.1002/2013JB010836.

Schultz, R., Stern, V., Novakovic, M., Atkinson, G. and Gu, Y.J. (2015a): Hydraulic fracturing and the Crooked Lake Sequences: insights gleaned from regional seismic networks; Geophysical Research Letters, v. 42, issue 8, p. 2750–2758, doi:10.1002/2015GL063455.

Schultz, R., Stern, V., Gu, Y.J. and Eaton, D. (2015b): Detection threshold and location resolution of the Alberta Geological Survey earthquake catalogue; Seismological Research Letters, v. 86, no. 2A, p. 385–397, doi:10.1785/0220140203.

Schultz, R., Corlett, H., Haug, K., Kocon, K., MacCormack, K., Stern, V. and Shipman, T. (2016): Linking fossil reefs with earthquakes: geologic insight to where induced seismicity occurs in Alberta; Geophysical Research Letters, v. 43, issue 6, p. 2534–2542, doi:10.1002/2015GL067514.

Schultz, R., Wang, R., Gu, Y.J., Haug, K. and Atkinson, G. (2017): A seismological overview of the induced earthquakes in the Duvernay play near Fox Creek, Alberta; Journal of Geophysical Research: Solid Earth, v. 122, issue 1, p. 492–505, doi:10.1002/2016JB013570.

Schultz, R., Atkinson, G., Eaton, D.W., Gu, Y.J. and Kao, H. (2018): Hydraulic fracturing volume is associated with induced earthquake productivity in the Duvernay play; Science, v. 359, issue 6373, p. 304–308, doi:10.1126/science.aao0159.

Skoumal, R.J., Brudzinski, M.R. and Currie, B.S. (2018): Proximity of Precambrian basement affects the likelihood of induced seismicity in the Appalachian, Illinois, and Williston Basins, central and eastern United States; Geosphere, v. 14, no. 3, p. 1365–1379, doi:10.1130/GES01542.1.

Stern, V.H., Schultz, R.J., Shen, L., Gu, Y.J. and Eaton, D.W. (2013): Alberta earthquake catalogue, version 1.0: September 2006 through December 2010; Alberta Energy Regulator, AER/AGS Open File Report 2013-15, 29 p.

Wetmiller, R.J. (1986): Earthquakes near Rocky Mountain House, Alberta, and their relationship to gas production facilities; Canadian Journal of Earth Sciences, v. 23, no. 2, p. 172–181, doi:10.1139/e86-020.